ISSN 1063-7745, Crystallography Reports, 2006, Vol. 51, No. 4, pp. 564–569. © Pleiades Publishing, Inc., 2006.
Original Russian Text © V.G. Kohn, 2006, published in Kristallografiya, 2006, Vol. 51, No. 4, pp. 605–610.

DIFFRACTION AND SCATTERING OF IONIZING RADIATIONS

Diffraction Reflection of a Focused X-ray Wave by a Multilayer Crystal

V. G. Kohn

Russian Research Centre Kurchatov Institute, pl. Akademika Kurchatova 1, 123182 Moscow
e-mail: kohn@kurm.polyn.kiae.su

Received February 2, 2006

Abstract—The Bragg diffraction of a narrow X-ray beam in a multilayer crystal is studied in the reflection geometry. It is shown by computer simulation of the experiment that strong integrated kinematic reflection occurs at any boundary of a multilayer crystal at the point of intersection of a narrow beam with the boundary. In contrast to the dynamic diffraction of a plane wave, attenuation of a narrow incident beam due to the reflection is small in comparison with the conventional absorption. As an example of a multilayer crystal, a Fabry–Perot interferometer is considered, which consists of two 70-μm-thick crystal Si layers separated by a 100-μm-thick air layer. The 12 4 0 reflection is studied at a photon energy of 15 keV. Three methods of formation of a narrow beam are considered: wavefront limitation by a slit, focusing with a parabolic lens, and focusing with a zone plate. It is shown that, for a local analysis of the thickness of layers and scattering parameters, the method of parabolic lens focusing has some advantages in comparison with the other methods.

PACS numbers: 61.10.Dp

DOI: 10.1134/S1063774506040043

INTRODUCTION

The general theory of the diffraction reflection of a spatially inhomogeneous X-ray wave in a single crystal was developed at the beginning of the 1970s. In [1–3], an analytic formula was derived for the amplitude of a diffracted wave at the output of a crystal for the case where a spherical wave from a point source located on the crystal surface enters the crystal. The function given by this formula, which is actually the propagator of the crystal, makes it possible to obtain a solution for an incident wave with an arbitrary wave front by calculating the convolution. The propagator of a crystal can be calculated by either solving the Takagi equations [1, 2] or direct integration of the reflection amplitude of a plane wave over the entire interval of angular deviations from the Bragg angle. Such an integration is equivalent to the calculation of the Fourier transform [3]. In the Laue geometry, where the diffracted wave passes into the crystal, the situation with a point source on the surface can be easily implemented using a narrow slit. This is a known scheme of section topography of individual defects in a crystal (see, for example, [4]). In the Bragg geometry, i.e., in the case of diffraction reflection, the use of a slit is unrealistic since the reflection is maximum specifically at the point of entrance of the incident wave into the crystal and the slit shuts in the detector.

In recent years, owing to development of X-ray focusing optics, a possibility arose to investigate the diffraction reflection from a source on the crystal surface by focusing a wave on the crystal surface rather than applying a slit. To this end, compound refractive lenses [5] are most appropriate (the parabolic profile [6], which provides the best focusing, is desirable). In the case of two-wave diffraction, planar lenses [7], which focus the wavefront only in the scattering plane, are quite appropriate. Moreover, since at symmetric diffraction a crystal does not change the beam width, the result is independent of a specific position of a crystal between the lens and detector. This circumstance makes it possible to place the detector exactly in the plane of the focus of the waves reflected from the crystal. In this case, in an experimental scheme with relatively large distances between the lens, crystal, and detector, the latter will record the same spatial dependence as if both the crystal and detector were located in the focus.

In [1–3], an analytic solution for the propagator was obtained for a crystal in the form of a plate of finite thickness. It was shown in [2] that fairly strong reflection occurs not only from the upper but also from the lower boundary of a crystal. Concerning multiple reflections from the boundaries, we should say that, although these reflections are taken into account in the analytic formulas, they are in fact very weak. This phenomenon has not been analyzed in detail. Physically, it is obvious that, in the case of a multilayer crystal, strong reflection should occur from each boundary; however, this situation has not been analyzed. The purpose of this study is to gain insight into this phenomenon. Numerical simulation of the symmetric diffraction

of a focused wave by a multilayer crystal is performed and the results obtained are qualitatively explained.

STATEMENT OF THE PROBLEM

The scheme of the numerical experiment is shown in Fig. 1. The point radiation source forms a divergent spherical wave. The X-ray lens, placed at the distance L_s from the source, focuses the spherical wave at the distance $L_f = F/(1 - F/L_s)$ from the lens, where F is the lens focal length. A multilayer crystal is placed on the path of the wave behind the lens. This crystal changes the direction of the optical axis, while deviating it by the double Bragg angle. Simultaneously, the crystal distorts the spatial distribution of the radiation field in the transverse direction (in the diffraction plane). For X rays, the paraxial approximation can be applied with high accuracy. Within this approximation, the Kirchhoff propagator $P(x, x', y, y', z)$ can be written as a product of two functions for the x (in the diffraction plane) and y (perpendicular to the diffraction plane) directions:

$$P(x, x', y, y', z) = P(x, x', z)P(y, y', z),$$
$$P(x, x', z) = \frac{1}{(i\lambda z)^{1/2}}\exp\left(i\pi\frac{(x - x')^2}{\lambda z}\right). \quad (1)$$

Here, the z axis is directed along the optical axis and λ is the X-ray wavelength. Within the paraxial approximation, the transport of the transverse dependence of the field along the optical axis is of interest. Since the polarization properties are insignificant, we will consider the scalar amplitude of the radiation field, assuming that the field is polarized in the plane perpendicular to the scattering plane. This situation can be easily implemented using synchrotron radiation. Since the crystal does not affect the dependence of the intensity on the coordinate y, we will consider only its dependence on x.

If the field amplitude $A(x)$ at a particular point on the optical axis is known, the transport of this field by a distance L is determined by the convolution with the function $P(x, x', L)$. Since the point source can be represented as a δ function, the intensity of the radiation from the point source at the distance L is equal to the propagator $P(x, 0, L)$. At the same time, we will assume the X-ray lens to be a thin object distorting the field amplitude in accordance with the laws of geometric optics. We can easily take into account the effects related to the lens length along the optical axis, since the analytic form of the propagator of a long lens is known [8]. However, for the effects related to the crystal, the specific features of a long lens are insignificant. Accordingly, the propagator of a parabolic planar refractive lens can be written as

$$P_{PRL}(x, x', z) = T_{PRL}(x)\delta(x - x'),$$
$$T_{PRL}(x) = \exp\left(-i\pi\frac{x^2}{\lambda F}[1 - i\gamma]\right). \quad (2)$$

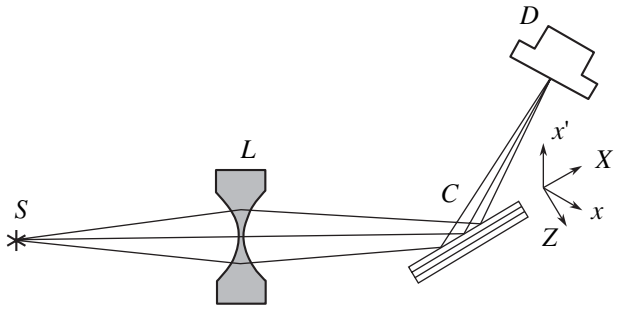

Fig. 1. Schematic of the numerical experiment: (*S*) point source of synchrotron radiation, (*L*) parabolic X-ray lens, (*C*) multilayer crystal, and (*D*) position-sensitive detector.

Here, $\delta(x)$ is the Dirac δ function, $\gamma = \beta/\delta$, the parameters δ and β determine the average complex polarizability of the lens material in accordance with the law $\chi_0 = -2\delta + 2i\beta$, and the focal length $F = R/2\delta$. As follows from (2), the lens changes the field amplitude locally at each point. The geometric aperture of the lens is not important, since the actual aperture is determined by the absorption.

Along with the parabolic planar lens, a zone plate can be used for focusing. In this context, it is of interest to compare the results of the numerical experiment performed with a parabolic lens and with a zone plate. In calculations, we used the expression for the propagator of a linear zone plate in the form

$$P_{ZP}(x, x', z) = T_{ZP}(x)\delta(x - x'),$$
$$T_{ZP}(x) = \exp(-i\varphi s(x)[1 - i\gamma]). \quad (3)$$

Here, $\varphi = K\delta t$ is the modulus of the phase shift of the wave passing through the material of the zones, $K = 2\pi/\lambda$, and t is the depth of the zone etch. The function $s(x)$ is equal to 1 at $r_1^2(2k) < x^2 < r_1^2(2k + 1)$ and beyond the zone plate aperture and is zero at $r_1^2(2k + 1) < x^2 < r_1^2(2k + 2)$. Here, r_1 is the radius of the first Fresnel zone, which determines the focal length in accordance with the law $F = r_1^2/\lambda$ and k is an integer in the interval from zero to the maximum number of zones.

The propagator of the diffraction reflection from the multilayer crystal, $P_{MC}(x, x', z)$, is also independent of z and, in the symmetric case, depends only on the difference in the arguments $(x - x')$, under certain conditions. Specifically, the coordinate x is counted from zero in the direction perpendicular to the deviated optical axis after the crystal, while the coordinate x' is counted in the direction perpendicular to the optical axis before the crystal. In addition, there is a coordinate system (X, Z) related to the crystal surface. Directions of the X and Z axes are shown in Fig. 1. The expression for the propa-

gator can be written as the Fourier integral

$$P_{MC}(x, x', z) = \int \frac{dq}{2\pi} R_{MC}(q) \exp(iq(x - x')). \quad (4)$$

The function $R_{MC}(q)$ is the reflection amplitude of a plane wave, a parameter that depends on the angular deviation (q/K) of the incident wave from the Bragg angle. This function is generally calculated with the recurrence formula (whose derivation can be found in many studies). Below, we give the expression obtained in [9], according to which $R_{MC}(q) = R_N(q)$, where the index N is the number of layers of a multilayer crystal. Accordingly, this function is obtained by multiple application of the recurrence formula

$$R_k(q) = \frac{R_1 - R_2 C \exp(i\varphi)}{1 - C\exp(i\varphi)}, \quad C = \frac{R_1 - R_{k-1}(q)}{R_2 - R_{k-1}(q)},$$
$$\varphi = \frac{ad_L}{\gamma_0}, \quad a = (\sigma^2 - s^2 f)^{1/2}, \quad R_{1,2} = \frac{\sigma \pm a}{sf}, \quad (5)$$
$$\sigma = (q - q_0)\sin 2\theta_B - i\mu_0, \quad s = K\chi_h,$$
$$f = \frac{\chi_{-h}}{\chi_h}, \quad \mu_0 = K\chi_0''.$$

Here, the designation x'' is used for the imaginary part of the complex quantity x and it is assumed that $a'' > 0$; d_L is the layer thickness; in the symmetric case, $\gamma_0 = \sin\theta_B$; and the parameters χ_0, χ_h, and χ_{-h} are the Fourier components of the crystal polarizability on the reciprocal lattice vectors **0**, **h**, and **–h**. The parameter $q_0 = K\varphi + K[\Delta E/E + \Delta d/d]\tan\theta_B$, where φ is the angle of rotation of the crystal from the exact position, $\Delta E/E$ is the relative change in the photon energy, and $\Delta d/d$ is the relative change in the interplanar spacing for reflecting atomic planes.

In general, rotation of the crystal changes the direction of the output optical axis and can be taken into account by introducing an additional exponential factor. In this study, we will assume that the crystal does not rotate. Concerning the changes in the photon energy and the interplanar spacing, the former parameter should be taken into account in the case of nonmonochromatic radiation and the latter can change from layer to layer. All parameters in formula (5) refer to the kth layer. It is assumed that the layers are enumerated from bottom to top, so that the first layer is the substrate and the upper boundary of the last layer is the input boundary of the crystal. Beginning with the function $R_0(q) = 0$ at $k = 0$ and consecutively applying formula (5), we obtain the necessary Fourier component of the propagator of a multilayer crystal at $k = N$.

Calculation of the spatial intensity distribution in the detector plane was performed by the method of double Fourier transformation using fast Fourier transformation [10] according to the following scheme. In the case of a parabolic lens, the field directly behind the lens is $A(x) = P(x, 0, L_s)\, T_{PRL}(x)$. The Fourier image $A^*(q)$ of this field was calculated. Furthermore, we used the property of a convolution of two functions, according to which its Fourier image is the product of the Fourier images of the multipliers. The function $A^*(q)$ was multiplied by the Fourier image of the Kirchhoff propagator $P^*(q, L_1)$ to take into account the distance L_1 between the lens and the crystal.

In a similar way, to take into account the crystal, a new multiplier (the function $R_{MC}(q)$) was added to the product. Finally, to take into account the last distance L_2 between the crystal and the detector, the multiplier $P^*(q, L_2)$ is necessary. With allowance for the analytic expression $P^*(q, z) = \exp(iz(q^2/2K))$, it can be easily shown that $P^*(q, L_1)P^*(q, L_2) = P^*(q, L_1 + L_2)$, and the result depends only on the total distance from the lens to the detector through the crystal. Thus, obtaining the Fourier image of the field at the detector in the form $B^*(q) = A^*(q)R_{MC}(q)P^*(q, L_1 + L_2)$ and calculating the inverse Fourier transform, we have the spatial field structure on the detector in the form of the function $B(x)$. The relative intensity was calculated with the formula $I(x) = |B(x)|^2\lambda(L_s + L_1 + L_2)$. In calculation of the Fourier images, the grid containing 65536 points with a uniform step of 0.02 μm was used.

As an example of a multilayer crystal, we will consider the Fabry-Perot interferometer that was designed and used in [11]. The interferometer consists of two 70-μm-thick crystal Si layers separated by a 100-μm-thick air layer. The input surface is parallel to the (3 1 0) planes. In [11], the reflection 12 4 0 was used, for which the Bragg angle is 90° at the photon energy E = 14.44 keV. In this study, we considered the same reflection, but the calculation was performed for E = 15 keV. In this case, the Bragg angle $\theta_B = 74.27°$. The other diffraction parameters in formula (5) are as follows: $\mu_0 = 2.254 \times 10^{-3}$ μm^{-1}, $s = (-2.486 + i0.1054) \times 10^{-2}$ μm^{-1}, and $f = 1$. These data were obtained using Stepanov's program [12].

DIFFRACTION OF A BEAM LIMITED BY A NARROW SLIT

Figure 2a shows the distribution of the relative intensity of a reflected wave in the case where the slit with the width D = 3 μm is installed at a distance of 50 m from the source and directly before the crystal. The distance between the crystal and the detector is also zero. In the limit of an infinitely narrow slit, the intensity distribution in the first two regions, i.e., after the point $x = 0$ of the entrance of the beam into the first layer and after the point $x = x_0$ of the emergence of the incident beam from the first layer, is described by the

analytical formula [2]

$$
\begin{aligned}
I(x) &= \left|\frac{sD}{2\sin 2\theta_B}\right|^2 \exp\left(-\mu_0 \frac{2x}{\sin 2\theta_B}\right) \\
&\times \left|\theta(x)G_0(x) - \theta(x-x_0)G_1(x)\right|^2, \\
G_0(x) &= J_0(Bx) + J_2(Bx), \\
G_1(x) &= J_0(B\eta) + 2\xi J_2(B\eta) + \xi^2 J_4(B\eta), \\
B &= \frac{(s^2 f)^{1/2}}{\sin 2\theta_B}, \quad x_0 = 2d_1 \cos\theta_B, \\
\eta &= (x^2 - x_0^2)^{1/2}, \quad \xi = \frac{x - x_0}{x + x_0}.
\end{aligned}
\tag{6}
$$

Here, $J_n(x)$ is the Bessel function of the first kind and nth order; $\theta(x)$ is a step function, equal to unity at a positive value of the argument and zero at a negative value; D is the slit width; and d_1 is the thickness of the first (crystalline) layer. Other designations are given in (5).

It is easy to make sure that the calculated curve is in agreement with formula (6). The maximum reflection at the point of entrance of the beam into the crystal is equal with good accuracy to the coefficient before the exponential in formula (6). Note that the behavior of the curve in the initial region is determined only by the upper boundary (specifically, by the reflection amplitude of the thick crystal at the tails of the angular dependence, where it is equal to $R(q) \approx s/2\sigma$). Indeed, taking into account only the tails, we have $I(x) = |DA_R(x)|^2$, where

$$
\begin{aligned}
A_R(x) &\approx \frac{s}{2\sin 2\theta_B}\int \frac{dq}{(2\pi)} \frac{\exp(iqx)}{(q - i\mu_0/\sin 2\theta_B)} \\
&= \frac{si}{2\sin 2\theta_B}\theta(x)\exp\left(-\frac{\mu_0 x}{\sin 2\theta_B}\right).
\end{aligned}
\tag{7}
$$

It follows from this formula that the measurement of relative intensity at the initial point makes it possible to directly determine the diffraction parameter $|\chi_h|$.

With an increase in x, the exponential law of the decrease in the intensity gradually transforms into a more complex law, in which multiple (dynamic) reflection becomes important. However, the lower layers do not manifest themselves. Finally, at the point x_0, the incident narrow beam reaches the lowest boundary. The presence of the boundary violates equilibrium and a new strong kinematic reflection with the opposite sign arises. Now, the function $G_1(0) = 1$. It is larger in magnitude than $G_0(x_0)$ and enters the sum with the opposite sign. In the limit of an infinitely narrow slit, the intensity directly behind the point x_0 is proportional to $|1 - G_0(x_0)|^2$. Therefore, the intensity sharply decreases if such a decrease has not occurred at a small layer thickness and, vice versa, increases if the intensity has significantly decreased at a large layer thickness. At the scattering parameters considered here, an intermediate situation also occurs. Since the curve was calculated for a nonzero slit, an additional specific feature arises. Specifically, there is a point near the boundary at which

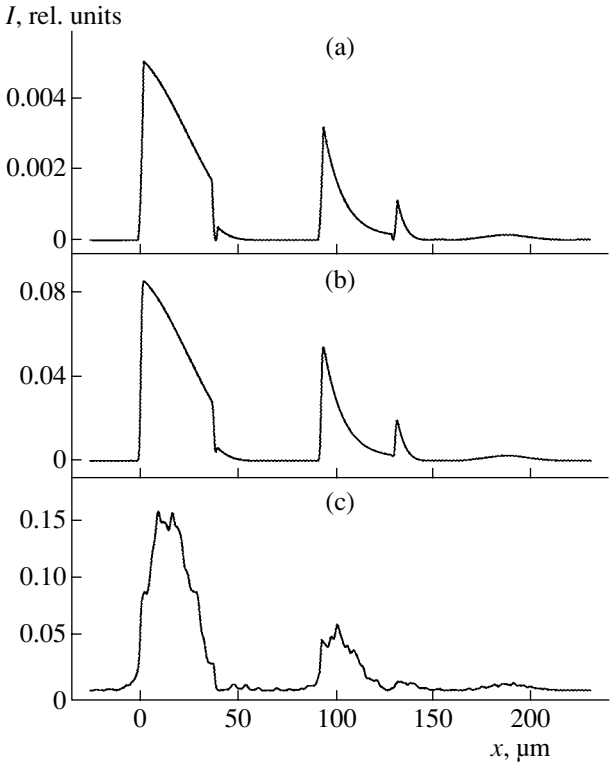

Fig. 2. Spatial distribution of the relative intensity on the detector in the case of reflection of a narrow beam by a multilayer crystal. The narrow beam is formed by (a) limitation of the wavefront by a narrow slit, (b) focusing by a parabolic lens, and (c) focusing by a Fresnel zone plate.

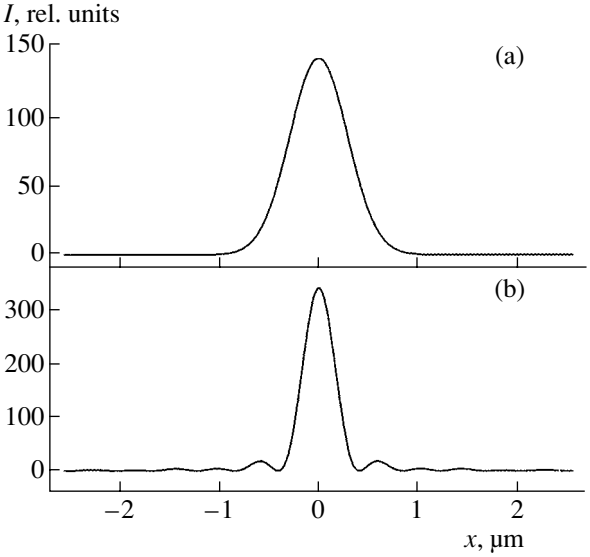

Fig. 3. Structure of the focal spot (point source image) for (a) a parabolic lens and (b) a zone plate.

both contributions compensate each other in the integration over the slit size and the intensity becomes zero.

With an increase in x in the second region, both contributions tend toward zero and the reflection disappears. However, the disappearance of the reflection does not mean the absence of the incident beam. In the sample under consideration, the second layer does not contain a crystal and does not reflect itself. Nevertheless, when the incident beam reaches the upper boundary of the third (crystalline) layer at the point $x_1 = x_0 + 2d_2\cos\theta_B$, where d_2 is the thickness of the second (air) layer, a new kinematic reflection arises. With an increase in x, the intensity decreases rapidly, as in the second region, although an analytic formula for this case has not been obtained. Finally, the intensity also changes stepwise at the intersection of the fourth sample boundary by the incident beam. It is interesting that the reflection maximum at the upper boundary of the second crystalline layer should be the same as for the first layer with allowance for the fact that the incident beam becomes weaker as a result of the absorption in the first layer and reflection. In the case under consideration, the complete decrease is determined by the coefficient 0.63, whereas the absorption factor is 0.72. This fact indicates that the intensity losses of the incident narrow beam caused by reflection are relatively low. The kinematic reflection tends toward zero as the distance between the reflection point and the boundary increases, independent of the incident-beam intensity. The reason for this phenomenon is that the waves reflected at different depths have different phases and, in total, reduce each other. Only the presence of the boundary violates the mutual extinction and results in a nonzero intensity of the reflected wave. This is the fundamental difference between the diffraction of a narrow beam and the dynamic diffraction of a plane wave. In the case of the reflection of a narrow beam, the dynamic diffraction (in the sense of the intensity transfer from the incident to the reflected beam) is absent. The reflected waves fall at the points in space where the incident beam is absent.

DIFFRACTION OF A BEAM FOCUSED BY A PARABOLIC LENS

As was noted above, a slit cannot be located directly before the crystal in the experiment with reflection. However, the use of a focusing lens meets no problems. In this section, we will discuss the results of the numerical experiment with the use of a parabolic X-ray lens. A schematic of the experiment is shown in Fig. 1. A biconcave silicon lens with the radius of curvature of the surfaces $R = 7.52$ μm was used in the calculations. According to [8], such a lens has the focal length F, the diffraction limit of the focus size s_f, and the effective aperture A determined by the formulas

$$F = \frac{R}{2\delta}, \quad s_f = 0.665(\lambda F\gamma)^{1/2}, \quad A = \left(\frac{\lambda F}{2\gamma}\right)^{1/2}, \quad (8)$$

where δ and γ were determined in (3). Substituting values of the parameters, we obtain $F = 174.2$ cm, $s_f = 0.66$ μm, and $A = 102.4$ μm. The intensity distribution in the focal region for a point source is shown in Fig. 3a.

Note that the experimentally measured focus size depends on the sizes of the source projection on the focal plane. In other words, it is necessary to calculate the convolution of the curve shown in Fig. 3a with a Gaussian having a half-width smaller than the effective size of the actual focus by a factor of L_f/L_s. However, upon reflection of the wave from the crystal, coherent diffraction from each point of the source occurs independently. Therefore, it is necessary to perform calculation with the point source and average the intensity recorded by the detector over the projection of the source size. In the calculation, the size of the source projection is 1 μm.

The results of the calculation of the reflection curve for a focused beam are shown in Fig. 2b. As follows from the calculation, the diffraction of the focused beam occurs in the same way as in the case with a slit. However, for a slit 0.7 μm in size, the intensity at the initial point is 0.0003, whereas in the case with the lens the intensity is 0.086, i.e., higher by a factor of 286. Hence, the gain in the intensity for the combination of a lens with a crystal is even larger than in the case of a single lens. Apparently, not only the maximum intensity in the focus but also the focus profile plays an important role. It is interesting that the averaging over the source size significantly affects the shape of the focus, whereas, in the case with the crystal, it is only slightly pronounced. The averaging leads only to the smoothing of the narrow dip in the intensity distribution near the lower boundary of the first crystal.

Thus, the use of a parabolic lens is effective in investigation of multilayer crystals since this technique makes it possible to measure the thicknesses of the layers locally at different points of the surface. One can change the Bragg angle, the order of reflection, and the wavelength in each specific case to obtain the most optimal conditions.

DIFFRACTION OF A BEAM FOCUSED BY A ZONE PLATE

Fresnel zone plates are often used in experiments to focus a beam. The result of the calculation in which the parabolic lens was replaced with a zone plate is shown in Fig. 2c. We used a linear silicon zone plate containing 226 zones; the radius of the first zone $r_1 = 12$ μm. The aperture of the zone plate is 360.8 μm. It was assumed that the zone plate has the maximum efficiency; i.e., the phase shift in the zones is equal to π. Since the zone plate lets radiation pass beyond the aper-

ture and the crystal completely reflects radiation, the region of the zone plate beyond the aperture was shut by the slit in order to obtain a pattern of higher quality. The focal length is the same as for the parabolic lens: $F = 174.2$ cm. The intensity distribution in the focal region for a point source is shown in Fig. 3b.

The calculation showed that a zone plate is not fit for the investigation of the reflection of a narrow beam from a crystal. In the case under consideration, a zone plate provides adequate focusing and even higher intensity in comparison with a parabolic lens owing to the large aperture. However, the radiation is focused within a large angular range, which significantly exceeds the angular range of the radiation reflected from the crystal. Therefore, the focus itself is reflected weakly. At the same time, a zone plate leaves a large part of the intensity beyond the focus owing to the presence of higher reflection orders. This intensity is distributed in space and, therefore, the beam cannot be considered narrow. In other words, higher focusing orders deteriorate the spatial structure of the wave reflected from a multilayer crystal.

Note that, in the case analyzed here, the distortion was very strong owing to the use of the high-order reflection (12 4 0), for which the width of the angular interval of strong reflection (the Bragg table) is $2|\chi_h|/\sin 2\theta_B = 1.25$ μrad. In the case of a wider Bragg table, we can obtain a curve closer to that shown in Fig. 2b. Nevertheless, the curve shape is always distorted. In addition, actual zone plates usually have a zero order (the phase shift is smaller than π). This circumstance deteriorates the situation even more. On the whole, we can conclude that zone plates are not fit for investigation of the local reflection from a multilayer crystal. Obviously, this conclusion does not concern different spectroscopic methods based on absorption of photons, in which the angular properties of a beam are not important.

ACKNOWLEDGMENTS

This study was supported by the Russian Foundation for Basic Research, project nos. 04-02-17363 and 05-02-16702.

REFERENCES

1. T. Uragami, J. Phys. Soc. Jpn. **27**, 147 (1969); **28**, 1508 (1970); **31**, 1141 (1971).
2. A. M. Afanas'ev and V. G. Kohn, Acta Crystallogr. A **27**, 421 (1971).
3. T. Saka, T. Katagawa, and N. Kato, Acta Crystallogr. A **28**, 102 (1972); **28**, 113 (1972); **29**, 192 (1973).
4. É. F. Suvorov, I. A. Smirnova, and E. V. Shulakov, Poverkhnost, No. 8, 67 (2005).
5. A. Snigirev, V. Kohn, I. Snigireva, and B. Lengeler, Nature **49**, 384 (6604) (1996).
6. B. Lengeler, C. G. Schroer, M. Kuhlmann, et al., J. Phys. D: Appl. Phys. **38** (10A), A218 (2005).
7. V. Aristov, M. Grigoriev, S. Kuznetsov, et al., Nucl. Instrum. Methods Phys. Res., Sect. A **470**, 131 (2001).
8. V. G. Kon, Zh. Éksp. Teor. Fiz. **124**, 224 (2003) [JETP **97**, 204 (2003)].
9. V. G. Kohn, Yu. V. Shvyd'ko, and E. Gerdau, Phys. Status Solidi B **221** (2), 597 (2000).
10. N. S. Bakhvalov, *Numerical Methods* (Nauka, Moscow, 1973; Mir, Moscow, 1977).
11. S.-L. Chang, Yu. P. Stetsko, M.-T. Tang, et al., Phys. Rev. Lett. **94**, 174 801 (2005).
12. http://sergey.gmca.aps.anl.gov.

Translated by A. Madonov